NANO LETTERS

Vibration-Assisted Electron Tunneling in C_{140} Transistors

A. N. Pasupathy,[†] J. Park,[†] C. Chang,[†] A. V. Soldatov,[‡] S. Lebedkin,[§]
R. C. Bialczak,[†] J. E. Grose,[†] L. A. K. Donev,[†] J. P. Sethna,[†] D. C. Ralph,[†] and
P. L. McEuen*,[†]

*Laboratory of Atomic and Solid State Physics, Cornell University,
Ithaca, New York 14853, Physics Department, Harvard University,
Cambridge, Massachusetts 02138, Department of Physics,
Luleå University of Technology, SE-971 87 Luleå, Sweden, and
Institut für Nanotechnologie, Forschungszentrum Karlsruhe,
D-76021 Karlsruhe, Germany*

ABSTRACT

We measure electron tunneling in transistors made from C_{140}, a molecule with a mass−spring−mass geometry chosen as a model system to study electron-vibration coupling. We observe vibration-assisted tunneling at an energy corresponding to the stretching mode of C_{140}. Molecular modeling provides explanations for why this mode couples more strongly to electron tunneling than to the other internal modes of the molecule. We make comparisons between the observed tunneling rates and those expected from the Franck−Condon model.

When electrons travel through molecules, vibrational modes of the molecules can affect current flow. Molecular-vibration-assisted tunneling was first measured in the 1960s using devices whose tunnel barriers contained many molecules.[1] Recently, effects of vibrations in *single* molecules have been measured using scanning tunneling microscopes,[2] single-molecule transistors,[3,4] and mechanical break junctions.[5] Theoretical considerations suggest that different regimes may exist depending on whether tunneling electrons occupy resonant energy levels on the molecule, and also on the relative magnitudes of the rate of electron flow, the vibrational frequency, and the damping rate of vibrational energy.[6−14]

A quantitative analysis of electron-vibration interactions has been difficult to achieve in previous molecular-transistor experiments. In transistors made from cobalt coordination complexes,[4] neither the precise nature of the vibrational modes nor their energies was determined independently of transport measurements. In transistors made from C_{60},[3] the "bouncing-ball" mode of a single C_{60} molecule against a gold surface was observed, a mode not intrinsic to the molecule itself. In this letter we study single-molecule transistors made using a molecule, C_{140}, with low-energy internal vibrational modes that are well understood. We observe clear signatures
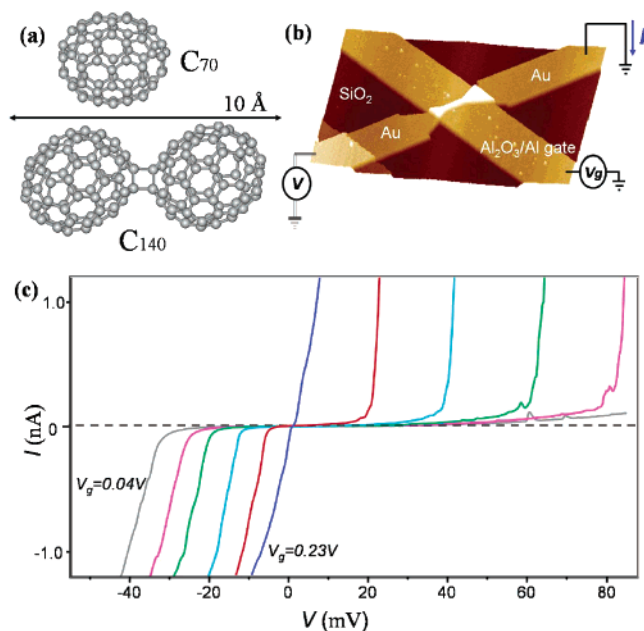
Figure 1. (a) C_{70} and C_{140}. (b) An atomic force microscope image of a continuous Au electrode, before we perform electromigration, fabricated on top of an oxidized Al gate electrode. (c) $I-V$ curves from a C_{140} single electron transistor for equally spaced values of V_g.

of one of these modes and discuss theoretically why it has the strongest coupling to tunneling electrons.

The C_{140} molecule consists of two C_{70} balls joined by two covalent C−C bonds (Figure 1a). The C_{140} we use was synthesized by pressure treatment of polycrystalline C_{70} at 1 GPa and 200 °C, purified by chromatography and characterized by C^{13} NMR, Raman, and infrared spectroscopy.[15] The vibrational modes of C_{140} have been measured by Raman spectroscopy and modeled numerically.[15] The six lowest-energy modes are intercage vibrations in which each C_{70} ball moves approximately as a rigid unit. The simple stretching mode is observed in Raman spectroscopy, with an energy of 11 ± 0.5 meV. The other intercage modes involve bending or twisting of the molecule, and they are predicted to be at 2.5, 2.7, 4, 15, and 17 meV. The lowest intracage excitation of C_{70} is ∼29 meV.[16]

An atomic force microscope image of our transistor structure is shown in Figure 1b. At least one C_{140} molecule bridges source and drain electrodes that are about 1 nm apart, with capacitive coupling to a gate electrode. To make these devices, we evaporate an Al pad 20 nm thick and 2 μm wide to serve as the gate and oxidize in air to form the gate insulator.[17,18] On top of the gate we pattern a gold wire 200−600 nm long, 20 nm high and 50−100 nm wide with 2−3 nm of Cr as an adhesion layer, or a platinum wire having a similar geometry without the adhesion layer. We then deposit approximately 10 μL of a 100 μM solution of C_{140} molecules in *o*-dichlorobenzene onto the device, and we allow the solvent to evaporate or we blow dry after approximately 10 min. After the molecules are deposited, we cool to cryogenic temperatures and use electromigration to create a nm-scale gap in the wire within which a molecule is sometimes trapped.[3,4,18,19] The success rate for incorporating a molecule

is approximately 10% for both the gold and platinum wires. The orientation of the molecule in the device is not known. All the measurements were performed either at 1.5 K or below 100 mK.

In Figure 1c, we show several current versus bias voltage ($I-V$) curves measured from a C_{140} device at different gate voltages (V_g). The device exhibits Coulomb-blockade behavior; electron flow is suppressed at low V because electrons must overcome a charging energy to tunnel. Plots of dI/dV as a function of V and V_g are shown in Figure 2a for four of the fourteen C_{140} devices we have examined. The dark areas on the left and right of each plot are regions of Coulomb blockade. The blockade energy barrier can be tuned with V_g to be >200 meV, the measurement limit set by electrode stability and noise at high V. Tunneling can occur close to $V = 0$ only near one value of gate voltage, V_c, which varies from device to device because of variations in the local electrostatic environment. Each of the C_{140} devices reported has only one accessible degeneracy point V_c. As long as we perform measurements close to $V_g = V_c$ we can be confident that the current flows through only a single charge state within one nanoscale object. While we cannot in principle rule out transport via a quantum state delocalized over a small number of C_{140} molecules, we see no nm-scale clustering of molecules when imaged by AFM. If we make devices using C_{140} solutions 100 times more concentrated, we commonly observe independent parallel tunneling through two or more molecules, as indicated by multiple degeneracy points at different V_g, with conductance signals indicating different ratios of capacitance to the source and drain electrodes.

The subject of this paper concerns the additional dI/dV lines that are observed in Figure 2a at values of $|V|$ larger than the boundary of the Coulomb-blockade regions. These lines correspond to thresholds involving excited quantum states of the molecule. The lines that meet the dark blockade area at $V_g < V_c$ ($V_g > V_c$) correspond to excited quantum levels of the $V_g < V_c$ ($V_g > V_c$) charge state. The energy of each level can be read from the bias voltage where the dI/dV line intercepts a boundary of the blockade region (white arrows).[3]

In Figure 2b, we plot a histogram of all of the excited-state energies that we resolve below 20 meV in fourteen C_{140} devices; excitations in each charge state are recorded separately. An excitation at 11 ± 1 meV is seen in eleven of the fourteen devices. In seven devices, the 11 meV line is present for both of the accessible charge states, while in four others it is seen for only one. In one sample (device I), well-resolved excited levels are also observed near 22 meV for both charge states, twice the 11 meV energy. As a control experiment, we measured eight devices made with C_{70} molecules. No prominent peak near 11 meV is present in the histogram of C_{70} levels (Figure 2c).

The presence of the 11 meV excitation in C_{140}, but not C_{70}, indicates that it is an excitation of the entire molecule, and not the C_{70} subunits. The presence of the same excitation for different charge states of the same molecule, and the observation of an excitation at 2 × 11 meV in one device, strongly suggest that the 11 meV excitation is vibrational in
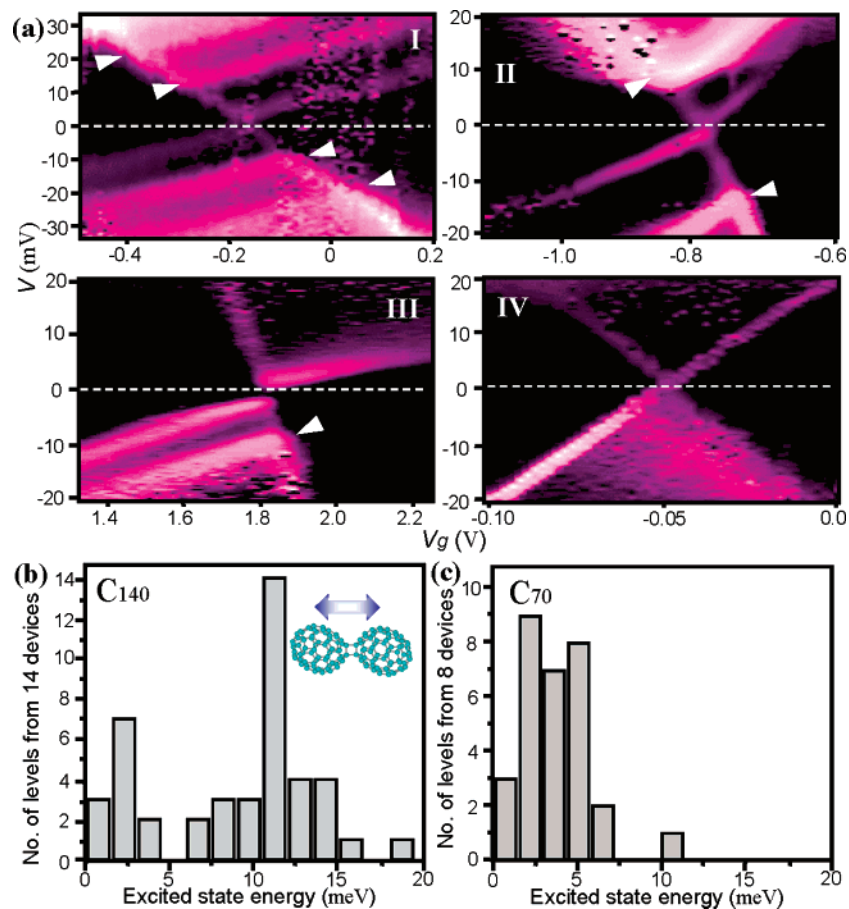
Figure 2. (a) dI/dV vs V and V_g for four C$_{140}$ devices. White arrows indicate excited levels at 11 and 22 meV. We include examples where the 11 meV levels are observed only in one charge state (III) and in neither state (IV). dI/dV is represented by a color scale from black (zero) to white (maximum), with maximum values 200 nS (device I), 600 nS (II), 15 nS (III), and 100 nS (IV). Measurements were done at 1.5 K for I−III and 100 mK for IV. (b) A histogram of observed excited energies from 28 charge states in 14 C$_{140}$ devices. (c) A similar histogram for eight C$_{70}$ devices.

nature. A purely electronic excitation should not be the same in both charge states, nor should it appear as multiples of a fundamental excitation. Based on its energy, we identify this excitation with the intercage stretch mode of C$_{140}$.[15] This is our principal result.

As shown in Figures 2b and 2c, additional excitations are present below 5 meV in both the C$_{140}$ and C$_{70}$ devices. For C$_{70}$, these are likely associated with the bouncing-ball mode of the molecule, as demonstrated previously for C$_{60}$.[3] The sub-5-meV excitations in C$_{140}$ devices might arise either from similar bouncing modes or from the intercage modes of C$_{140}$ at 2.5, 2.7, and 4 meV. However, calculations (below) suggest that the tunneling electrons couple strongly only to the intercage stretch mode, not the other internal modes. We do not observe peaks in the C$_{140}$ histogram near the bending/twisting intercage modes at 15 and 17 meV.

We will analyze our data within the framework of the Franck−Condon model.[20] C$_{140}$ has a large number of vibrational states we denote by α_j, where α labels the mode of frequency ω_α and j is the number of vibrational quanta excited in the mode. For each vibrational mode, the tunneling electron drives a transition from the ground vibrational state with A electrons to a vibrational state α_j with B electrons, where $B - A = +1(-1)$ for tunneling on (off) the molecule. The tunneling rate is determined by the overlap of the starting

configurational wave function, Ψ_g^A, with the one after tunneling, $\Psi_{\alpha j}^B$:

$$\Gamma_{\alpha j}^{A \to B} = \Gamma_{electron} P_{\alpha j} \qquad (1)$$

where

$$P_{\alpha j} = |\langle \Psi_{\alpha j}^B | \Psi_g^A \rangle|^2 \text{ and } \sum_j P_{\alpha j} = 1$$

If the electronic contribution $\Gamma_{electron}$ is assumed constant for the different vibrational transitions and if the rate-limiting step for current flow is the $A \to B$ transition, the current step associated with a given vibrational excitation is

$$\Delta I_{\alpha j}/\Delta I_g = P_{\alpha j}/P_g \qquad (2)$$

where ΔI_g is the ground-state current. To predict the size of the current steps, we must therefore calculate the atomic rearrangements that occur when a charge is added to or subtracted from the molecule. We will first perform this calculation for an isolated C$_{140}$ molecule and then discuss the effects of the local electrostatic environment, before making comparisons to our measurements.

For the isolated molecule, we calculate the overlaps $P_{\alpha j}$ using the semiempirical method PM3 under Gaussian 03.[21]
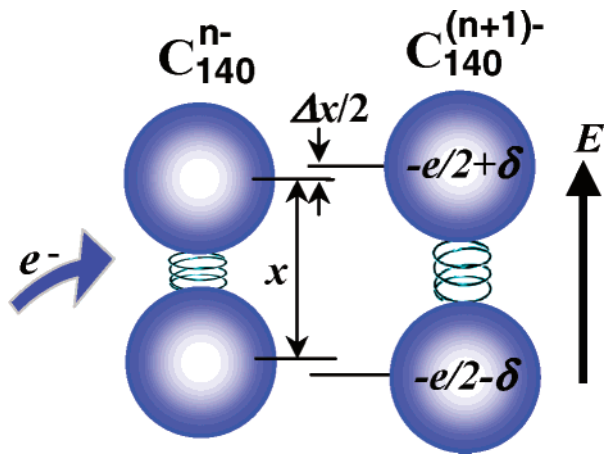
Figure 3. One possible mechanism for the field-enhanced excitation of the intercage vibrational mode.

Figure 4. Values of $I_{11\text{meV}}/I_g$, the measured current step for the excited-state signal relative to the ground-state current. Values for both charge states n^- (squares) and $(n + 1)^-$ (diamonds) are shown. One value is not displayed: for device XII, $I_{11\text{meV}}/I_g = 8 \pm 2.5$ for the $(n + 1)^-$ charge state. Samples IV, XIII, and XIV have no visible 11 meV levels.

The charge state of C_{140} in our devices is not known, but since the fullerenes are easily reduced and not easily oxidized,[22] we have analyzed the initial charge states $n^- = 0$, 1^-, 2^-, and 3^-. The PM3 calculations indicate that the probability of tunneling without exciting any of the vibrational degrees of freedom is small. This means that tunneling at low biases is suppressed. The coupling is distributed over all of the vibrational modes, but it is large for a relatively small number. Within our measurement range (eV < 30 meV), the calculations indicate that the coupling is dominated by a single mode, the 11 meV stretching mode ($\alpha = s$). For the $0 \rightarrow 1^-$ transition, $P_{s1}/P_g = 0.25$. Couplings to all other vibrational modes in the measurement range are found to be smaller by at least a factor of 10. The results are qualitatively similar for other charge states.

The physics of the 11 meV stretching mode can be captured using a simple model of the molecule with two masses $M/2$ connected by a spring with a spring constant k, as illustrated in Figure 3. The vibrational frequency is $\omega_s = (4k/M)^{1/2}$ and the zero-point rms amplitude of fluctuations in the vibrational coordinate is $x_o = [2\hbar/(M\omega)]^{1/2} = 2$ pm.[20] The length of the molecule changes by Δx when one charge is added. The Franck–Condon result for the transition probability associated with one quantum of the stretching mode, normalized by the ground-state probability, is

$$Ps_1/Pg = (\Delta x/x_0)^2/4 \qquad (3)$$

Higher-order transitions involving j quanta of a vibrational mode have rates related to the one-quantum transitions:[20]

$$P_{sj}/P_g = (P_{s1}/P_g)^j/j! \qquad (4)$$

In going from the neutral to 1^- charge state for isolated C_{140}, PM3 predicts that $\Delta x = -1.9$ pm. Equation 3 then gives $I_{s1}/I_g = 0.23$, in good agreement with the full calculation above. Multiple-quanta transitions should be much smaller by eq 4. For other charge states, the calculated strength of the transition assisted by the stretching mode is weaker, because Δx is smaller: for the $1^- \rightarrow 2^-$ transition $\Delta x = -0.4$ pm, for $2^- \rightarrow 3^-$ $\Delta x = -0.1$ pm, and for $3^- \rightarrow 4^-$ $\Delta x = -0.3$ pm.
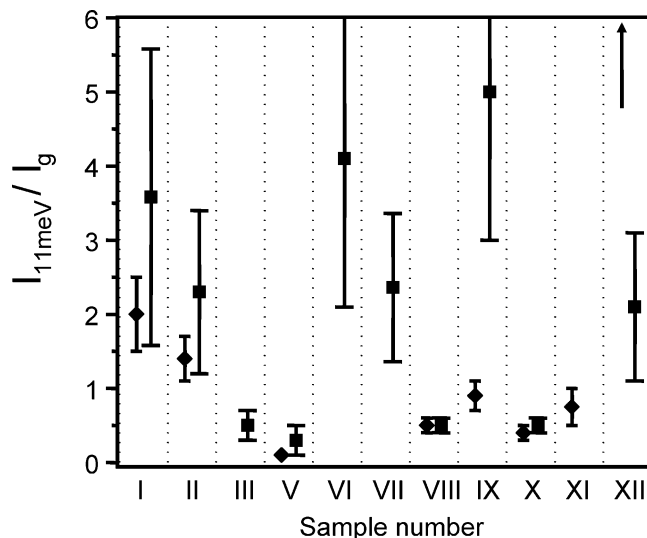
The electrostatic environment in the neighborhood of the C_{140} molecule may also play an important role in determining vibration-assisted tunneling rates. In general, we expect that the C_{140} molecule will be subject to a strong local electric field E due to image charges, work-function differences, and/or localized charged impurities. For example, an image charge at a distance 0.8 nm generates $E = 2$ V/nm. We have not succeeded in making quantitative estimates of these field-enhancement effects because the Gaussian 03 implementation of PM3 does not allow for solutions in an external field. However, a local field can be expected to preferentially enhance vibration-assisted tunneling associated with the stretching mode. When an extra electron tunnels onto C_{140}, the presence of E will produce unequal charges on the two C_{70} cages, as illustrated in Figure 3. The rearrangement of charge density within the molecule will produce changes in chemical bonding forces, leading to changes in Δx. In addition, the interaction of E with the charge polarization ($+\delta$, $-\delta$ in Figure 3) will stretch the C_{140} by a length $\Delta x = E\delta/k$. To estimate the magnitude of this stretching, assume that the charge is fully polarized: $\delta = e/2$, and $E = 2$ V/nm. Then the electrostatic stretching is $\Delta x \sim 1$ pm. Both this stretching and the chemical-bonding rearrangement might produce displacements of magnitude comparable to the values calculated above for isolated C_{140}. Such electric-field effects should depend strongly on the angle between the field and the molecular axis, because C_{140} is most easily polarized along its long axis.

Figure 4 shows the measured ratio $\Delta I_{s1}/\Delta I_g$ for both charge states n^- and $(n + 1)^-$ of each device, determined by taking the ratio of the current-step height at the 11 meV peak to I just before the step. An increasing overall background was also observed that gives uncertainties in the step heights. In five of the devices (I, II, V, VIII, and X), the ratios were the same in both charge states, as expected within the simple

Franck−Condon picture if the vibrational energies are not altered significantly by the addition of an electron. In three of these devices, $\Delta I_{s1}/\Delta I_g < 0.6$, small enough to be consistent with the PM3 estimates above. Only the $j = 1$ vibrational state was observed for these three devices, in agreement with theory. For device I, $\Delta I_{s1}/\Delta I_g = 3.6 \pm 2.0$ and 2.0 ± 0.5 for the n^- and $(n + 1)^-$ states, respectively, indicating stronger coupling than expected from our estimate for isolated C_{140}. For this sample, additional lines were observed corresponding to the emission of two vibrational quanta ($j = 2$) with amplitudes $\Delta I_{s2}/\Delta I_g = 7.3 \pm 4$ for the n^- charge state and 2.3 ± 1.5 for the $(n + 1)^-$ charge state. Equation 4 predicts 6.5 ± 4 and 2 ± 1 respectively, in good agreement with the measurements. For device II, strong coupling was also observed, but no $j = 2$ line was resolved, although the increasing background may have masked its presence. Overall, then, this subset of five devices is in reasonable agreement with the Franck−Condon predictions.

In the other devices showing an 11 meV feature, we observed behaviors that are unexpected in our simple Franck−Condon picture. Large differences were observed in $\Delta I_{s1}/\Delta I_g$ for the two charge states; sometimes a line was present for only one charge state (devices III, VI, VII, and XI). In addition, anomalously large values of $\Delta I_{s1}/\Delta I_g$ were observed. These could either reflect strong electron−phonon coupling or an anomalous suppression of tunneling into the ground state by vibrational or other phenomena. Pronounced negative differential resistance was present in one device (VI).[8,9]

In summary, in transistors made from C_{140} we observe vibration-assisted tunneling associated with an internal stretching mode of the molecule. The strong coupling of this mode to tunneling electrons, relative to the other molecular modes, is consistent with molecular modeling. Variations in the measured strength of vibration-assisted tunneling between different devices may be associated with an enhancement of the coupling between tunneling electrons and stretching-mode excitations by local electric fields.

References

(1) Jaklevic, R. C.; Lambe, J. *Phys. Rev. Lett.* **1966**, *17*, 1139.
(2) Stipe, B. C.; Rezaei, M. A.; Ho, W. *Science* **1998**, *280*, 1732.
(3) Park, H.; et al. *Nature* **2000**, *407*, 57.
(4) Park, L.; et al. *Nature* **2002**, *417*, 722.
(5) Smit, R. H. M.; et al. *Nature* **2002**, *419*, 906.
(6) Glazman, L. I.; Shekhter, R. I. *Zh. Eksp. Teor. Fix.* **1988**, *94*, 292; *Sov. Phys. JETP* **1988**, *67*, 163.
(7) Gorelik, L. Y.; et al. *Phys. Rev. Lett.* **1998**, *80*, 4526.
(8) Boese, D.; Schoeller, H. *Europhys. Lett.* **2001**, *54*, 668.
(9) McCarthy, K. D.; Prokof'ev, N.; Tuominen, M. T. *Phys. Rev. B* **2003**, *67*, 245415.
(10) Zhu, J.-X.; Balatsky, A. V. *Phys. Rev. B* **2003**, *67*, 165326.
(11) Mitra, A.; Aleiner, I. L.; Millis, A. J. cond-mat/0302132.
(12) Flensberg, K. *Phys. Rev B* **2003**, *68*, 205323. Braig, S.; Flensberg, K. *Phys. Rev. B* **2003**, *68*, 205324.
(13) Aji, V.; Moore, J. E.; Varma, C. M. cond-mat/0302222.
(14) Zhitenev, N. B.; Meng, H.; Bao, Z. *Phys. Rev. Lett.* **2002**, *88*, 226801.
(15) Lebedkin, S.; Hull, W. E.; Soldatov, A.; Renker, B.; Kappes, M. M. *J. Phys. Chem. B* **2000**, *104*, 4101.
(16) Dresselhaus, M. S.; Dresselhaus, G.; Eklund, P. C. *Science of Fullerenes and Carbon Nanotubes*; Academic: New York, 1996.
(17) Persson, S. H. M.; Olofsson, L.; Gunnarsson, L. *Appl. Phys. Lett.* **1999**, *74*, 2546.
(18) Liang, W.; Shores, M. P.; Bockrath, M.; Long, J. R.; Park, H. *Nature* **2002**, *417*, 725.
(19) Park, H.; Lim, A. K. L.; Alivisatos, A. P.; Park, J.; McEuen, P. L. *Appl. Phys. Lett.* **1999**, *75*, 301.
(20) Schatz, G. C.; Ratner, M. A. *Quantum Mechanics in Chemistry*; Prentice Hall: Englewood Cliffs, NJ, 1993.
(21) Frisch, M. J.; Trucks, G. W.; Schlegel, H. B.; Scuseria, G. E.; Robb, M. A.; Cheeseman, J. R.; Montgomery, J. A., Jr.; Vreven, T.; Kudin, K. N.; Burant, J. C.; Millam, J. M.; Iyengar, S. S.; Tomasi, J.; Barone, V.; Mennucci, B.; Cossi, M.; Scalmani, G.; Rega, N.; Petersson, G. A.; Nakatsuji, H.; Hada, M.; Ehara, M.; Toyota, K.; Fukuda, R.; Hasegawa, J.; Ishida, M.; Nakajima, T.; Honda, Y.; Kitao, O.; Nakai, H.; Klene, M.; Li, X.; Knox, J. E.; Hratchian, H. P.; Cross, J. B.; Adamo, C.; Jaramillo, J.; Gomperts, R.; Stratmann, R. E.; Yazyev, O.; Austin, A. J.; Cammi, R.; Pomelli, C.; Ochterski, J. W.; Ayala, P. Y.; Morokuma, K.; Voth, G. A.; Salvador, P.; Dannenberg, J. J.; Zakrzewski, V. G.; Dapprich, S.; Daniels, A. D.; Strain, M. C.; Farkas, O.; Malick, D. K.; Rabuck, A. D.; Raghavachari, K.; Foresman, J. B.; Ortiz, J. V.; Cui, Q.; Baboul, A. G.; Clifford, S.; Cioslowski, J.; Stefanov, B. B.; Liu, G.; Liashenko, A.; Piskorz, P.; Komaromi, I.; Martin, R. L.; Fox, D. J.; Keith, T.; Al-Laham, M. A.; Peng, C. Y.; Nanayakkara, A.; Challacombe, M.; Gill, P. M. W.; Johnson, B.; Chen, W.; Wong, M. W.; Gonzalez, C.; Pople, J. A. *Gaussian 03*, revision A.1; Gaussian, Inc.: Pittsburgh, PA, 2003.
(22) Echegoyen, L.; Echegoyen, L. E. *Acc. Chem. Res.* **1998**, *31*, 593.